Wagner, G., Kumar, A., & Wüthrich, K. (1984) *Eur. J. Biochem. 114*, 375-384.
Weaver, D. T., & DePamphilis, M. L. (1984) *J. Mol. Biol. 180*, 961-986.
Weiner, S. J., Kollman, P. A., Nguyen, D. T., & Case, D. A. (1986) *J. Comput. Chem. 7*, 230-235.
Wider, G., Macura, S., Kumar, A., Ernst, R. R., & Wüthrich, K. (1984) *J. Magn. Reson. 56*, 207-234.

Characterization of the Overall and Internal Dynamics of Short Oligonucleotides by Depolarized Dynamic Light Scattering and NMR Relaxation Measurements†

Wolfgang Eimer, James R. Williamson,‡ Steven G. Boxer, and R. Pecora*
Department of Chemistry, Stanford University, Stanford, California 94305-5080
Received July 10, 1989; Revised Manuscript Received September 1, 1989

ABSTRACT: The dynamics of three synthetic oligonucleotides $d(CG)_4$, $d(CG)_6$, and d(CGCGTTGTTCGCG) of different length and shape were studied in solution by depolarized dynamic light scattering (DDLS) and time-resolved nuclear Overhauser effect cross-relaxation measurements. For cylindrically symmetric molecules the DDLS spectrum is dominated by the rotation of the main symmetry axis of the cylinder. The experimental correlation times describe the rotation of the oligonucleotides under hydrodynamic stick boundary conditions. It is shown that the hydrodynamic theory of Tirado and Garcia de la Torre gives good predictions of the rotational diffusion coefficients of cylindrically symmetric molecules of the small axial ratios studied here. These relations are used to calculate the solution dimensions of the DNA fragments from measured correlation times. The hydrodynamic diameter of the octamer and dodecamer is 20.5 ± 1.0 Å, assuming a rise per base of 3.4 Å. The tridecamer, d(CGCGTTGTTCGCG), adopts a hairpin structure with nearly spherical dimensions and a diameter of 23.0 ± 2.0 Å. The DDLS relaxation measurements provide a powerful method for distinguishing between different conformations of the oligonucleotides (e.g., DNA double-helix versus hairpin structure). Furthermore, the rotational correlation times are a very sensitive probe of the length of different fragments. The NMR results reflect the anisotropic motion of the molecules as well as the amount of local internal motion present. The experimental correlation time from NMR is determined by the rotation of both the short and long axes of the oligonucleotide. The contributions of the various correlation times are given by the relative orientation of the internuclear vector with respect to the main axis and the correlation function for internal motion, if it is assumed that the librational motions decay much faster than the overall reorientational motion. Our results are compared with those from NMR relaxation measurements on other short oligonucleotides with lengths of up to 20 base pairs. Various dynamic models for the reorientation of the internuclear vector are applied to their interpretation. The extent of local internal motion is apparently independent of the length and base sequence of the DNA fragments and gives a significant contribution to the effective correlation time measured by the cross-relaxation rate.

The biological function of DNA and RNA is most likely determined not only by sequence-dependent properties and static conformation but also by its dynamics. DNA is a semiflexible macromolecule and, due to its length, exhibits a complex dynamic behavior. The local internal motions of DNA have become the subject of increasing interest in recent years. Fast fluctuations in the conformation of DNA may play an important role in transcription and the DNA-protein recognition process. The conformational fluctuations occur on a time scale between 10^{-6} and 10^{-12} s and include long-range twisting and bending motions as well as very local fluctuations of small segments about an equilibrium position. Experiments using various types of probes, mainly time-resolved fluorescence polarization anisotropy (FPA) (Genest & Wahl, 1978; Barkley & Zimm, 1979; Millar et al., 1981; Magde et al., 1983), ESR (Bobst et al., 1984; Kao & Bobst, 1985), and NMR[1] relaxation experiments of different nuclei (Early & Kearns, 1979; Bolton & James, 1980a,b; Hogan & Jardetzky, 1980; Mirau & Kearns, 1983; Assa-Munt et al., 1983; Mirau et al., 1985), have been performed to characterize the nanosecond to subnanosecond motions. The fluorescence depolarization measurements show a very rapid initial decay which could be partially resolved by using a picosecond laser setup (Magde et al., 1983). The very fast decay was attributed to the "wobbling" of the intercalated dye molecules (Barkley & Zimm, 1979) with a root mean square fluctuation of about ±21°. ESR and NMR studies confirmed the existence of librational motions for the bases and other segments in polynucleotides. The time scale and especially the amplitude for the relaxation processes have been the subject of controversy (Hård, 1987; Schurr & Fujimoto, 1988). For an unambiguous interpretation of NMR and ESR results, it is necessary to provide a precise theory that accounts for the rather complex dynamics of the long DNA fragments, where it is expected that different relaxation modes couple. When collective twisting and bending motions are neglected, the experimental

† This work was supported by a grant from the National Institutes of Health (R01 GM27738) to S.B. and a grant from the National Science Foundation (CHE-88-14641) to R.P. Further support came from the NSF-MRL program through the Center for Materials Research at Stanford University.
‡ Present address: Department of Chemistry and Biochemistry, University of Colorado, Boulder, CO 80309.

[1] Abbreviations: NMR, nuclear magnetic resonance; DDLS, depolarized dynamic light scattering; NOE, nuclear Overhauser enhancement.

0006-2960/90/0429-799$02.50/0

results indicate a rather large amplitude of about 35° and in some cases even larger values. Taking into account the long-range fluctuations, Schurr and Fujimoto (1988) estimated the amplitude of the local motion of bases to reduce to ≈10°.

A knowledge of the extent of internal motion and the overall molecular reorientation is also an important precondition for determining the structure of oligonucleotides by 2D NMR (Wüthrich, 1986; Borgias & James, 1988) in solution. There is experimental evidence that the structure in a crystal or fiber differs significantly from the conformation of very short DNA fragments in solution. For B-DNA, X-ray crystallography data (Saenger, 1984) indicates that the base planes are oriented nearly perpendicular to the helix axis; the tilt angle varies mostly between 0 and 5°. On the other hand, linear dichroism spectroscopic studies (Edmondson & Johnson, 1985, 1986, 1987) and electric dichroism measurements (Hogan et al., 1979) of the conformation of polynucleotides in solution predict a tilt angle that may be even greater than 25° and depends on the base-pair sequence. These findings have been questioned (Lee & Charney, 1982; Charney et al., 1986), and it is still not clear whether or not the structural parameters in solution differ from those in crystals. A large-amplitude internal motion would complicate any structure determination using distance information obtained from 2D NMR spectroscopy. Criticism in this direction has already been raised on the basis of the experimental finding of some very large librational amplitudes of the bases. A better understanding of relaxation mechanisms within DNA fragments is therefore essential for the justification of the complex structure determination procedures.

Depolarized dynamic light scattering (DDLS) and NMR cross-relaxation studies are combined here for the first time to characterize the overall and internal motions of a set of small DNA fragments. The shapes used for calculating hydrodynamic properties of the oligonucleotides can be approximated as axially symmetric bodies such as ellipsoids or cylinders. DDLS spectra are determined by the reorientational motion of the symmetry axis of the oligonucleotides, which is the end-over-end rotation. The size of the cylindrical molecules can be calculated from a knowledge of the experimental rotational diffusion coefficient. A theory for the translational and rotational diffusion coefficients of cylindrically symmetric molecules with a large length-to-diameter ratio was developed by Broersma (Broersma, 1960a,b; 1980) almost 30 years ago. This theory is, however, not applicable to the transport coefficients of short cylinders. A more recent hydrodynamic model by Tirado and Garcia de la Torre (Tirado & Garcia de la Torre, 1979, 1980) overcomes this problem and gives expressions for D the translational and Θ the rotational diffusion coefficient of rodlike molecules in the range $2 \leqslant p \lesssim 30$, where $p = L/d$, the length to diameter ratio. The hydrodynamic behavior of relatively long DNA fragments ($p \approx 25$) is well described by this theory (Tirado et al., 1984a). For low values of p the theory also gives good agreement with experimental data (Tirado et al., 1984b). Furthermore, the hydrodynamic theory can be used to calculate an effective rotational correlation time for a rigid, anisotropic molecule, where motions about the different axes have to be considered. The NMR cross-relaxation experiment monitors the reorientation of the cylindrical molecules about both the long and short molecular symmetry axes (Huntress, 1968). In the NMR experiments three different correlation times contribute to the measured effective correlation time for a cylindrically symmetric molecule. The relative contributions of these times depend on the orientation of the internuclear vector whose relaxation is being studied with respect to the main symmetry axis of the cylinder. In addition, any internal motion of the internuclear vector in the molecular frame also contributes to the spectral density. Assuming that the librational motions of the bases take place on a much faster time scale than the overall motion, the internal motion affects the relative contributions of the three rotational correlation times, i.e., has an influence on the amplitude factors.

To characterize the internal motion of DNA, long fragments with a length of more than 100 base pairs have usually been studied. This has the disadvantage that the relaxation mechanism for such long molecules is in general complex. The fragments are relatively flexible, and therefore, besides local internal motions of the bases and the backbone, collective twisting and bending motions also have to be considered. This makes a straightforward interpretation of the experimental data more difficult. To mitigate this complication, we have studied the very short oligonucleotides $d(CG)_4$ and $d(CG)_6$, 8 and 12 base pairs long, for which collective motions are likely to be less important. These molecules are well approximated by cylinders. Furthermore, we have studied d-(CGCGTTGTTCGCG), which adopts a specific hairpin structure (Williamson & Boxer, 1989). Under these conditions the molecule is almost spherical and the overall reorientational motion should be different from that of the corresponding helical duplex molecules.

DNA has been found to exist in several different conformations in vitro and in vivo. These include, A-, B-, and Z-DNA as well as bent or hairpin structures. The biological importance of some of the conformations has not yet been clarified. It is, however, of great interest to develop spectroscopic methods that can identify conformational differences of DNA oligomers to facilitate the study of possible structure–activity relationships. In the following we show that DDLS is a very powerful tool for distinguishing between the duplex and hairpin DNA forms. In addition, it can be used to measure small changes in DNA length such as those that might occur by intercalation.

In contrast to FPA and ESR experiments, no introduction of a label molecule or a chemical modification of the bases is necessary in the case of DDLS. Thus, any uncertainty about possible structural changes upon chemical modification and the orientation of the transition moment (FPA) or hyperfine principal axes (ESR) is avoided. The interpretation of DDLS experimental results is relatively straightforward. The line width of the depolarized spectrum directly gives the reorientational relaxation time of the rotation about the short symmetry axes. Any pair correlation effect, which might occur because DDLS is a coherent process, can be accounted for by performing the measurements as a function of concentration.

In general, NMR relaxation experiments have the disadvantage that the spectral density and therefore the relaxation rate depends on r^{-6}, the inverse sixth power of the internuclear distance. Often r is not known and may change during the reorientational motion. This problem was avoided in our experiments because we followed the buildup of NOE from the H6 to the H5 of the cytosine bases. The position of the protons is fixed within the aromatic ring, and their distance is well-known. For a rigid cylindrical body the effective correlation time that determines the spectral density can be calculated by using Woessner's formalism (Woessner, 1962). To account for local internal motion Lipari and Szabo (1982a,b) have proposed a general theory that they call a "model-free approach". The assumption is that the internal motion is much faster than the overall reorientation and that

the decay of the internal motion is characterized by a single exponential. In this model the information about the fast component of the relaxation parameter in a NMR experiment can be described by a "generalized order parameter" S, which reflects the spatial restrictions of the internal motion, and an internal correlation time τ_{int}, which characterizes the frequency of the motion. S^2 is the asymptotic value of the normalized internal autocorrelation function for $t = \infty$. It is also possible to construct dynamic models for the internal motion, derive the correlation function, and obtain more information about the geometric restrictions of the motion. One approach is the diffusion in a cone model (Lipari & Szabo, 1981), for which Wang and Pecora (1980) have calculated the time correlation functions. Another model assumes that the system undergoes overdamped librational motions (Schurr & Fujimoto, 1988; Schurr, 1984) about an equilibrium position in harmonic polar and azimuthal potential wells. We have applied all three models to our data and give a comparison of the final results.

In the following section, a brief summary of some of the relevant underlying principles of DDLS and NMR cross-relaxation experiments is given to show the strengths and weaknesses of each technique and how they may be used to complement each other in studying the dynamics of short DNA fragments.

Theory

For rigid molecules both spectroscopic methods, DDLS and NMR relaxation, monitor directly or indirectly the time dependence of a stochastic variable R, which is a function of the orientation angles Ω of the molecules. The time dependence of $R(t)$ is characterized by its time autocorrelation function

$$C(t) = \langle R(t)R(0)\rangle \tag{1}$$

where the the angular brackets indicate an ensemble average. The stochastic variable R that determines the time correlation function in a given experiment, for example, the polarizability tensor α in DDLS or the dipolar interaction between two nuclei in NMR relaxation experiments, may be expressed in terms of linear combinations of the Wigner rotation matrices of $J = 2$ with coefficients containing the spherical tensor components of the particular stochastic variable in the molecule-fixed frame. These molecule-fixed spherical tensor components are time independent for rigid molecules. The Wigner rotation matrices express the time-dependent transformation of R from the molecule-fixed frame to the laboratory-fixed frame. The correlation functions of interest for our experiments are thus linear combinations of time correlation functions of the form

$$C(t) = \langle D^{(2)*}{}_{k,m}[\Omega_{LF}(0)]D^{(2)}{}_{k,m}[\Omega_{LF}(t)]\rangle \tag{2}$$

where Ω_{LF} denotes the Euler angles that specify the orientation of the molecule in the laboratory-fixed system. The relevant linear combinations consist in general of a sum of five exponentials

$$C(t) = \sum_m A_m \exp-(t/\tau_m) \tag{3}$$

where the sum is over $m = 0, \pm1$, and ±2. The τ_m for rigid cylindrically symmetric molecules is given in terms of $\Theta_\perp$ and $\Theta_\parallel$, the rotational diffusion coefficients for the reorientation about the short and long axes of the cylinder, respectively: $1/\tau_m = 6\Theta_\perp + m^2(\Theta_\parallel - \Theta_\perp)$. The τ_m's are the same for both spectroscopic techniques, but the amplitude factors A_m are specific for the DDLS and the NMR experiments and are responsible for the differences in the experimental information obtained from them.

In the case of DDLS the time autocorrelation function of the scattered light electric field is determined by the laboratory-fixed yz component of the polarizability tensors α of the molecules (Berne & Pecora, 1976). For asymmetric molecules, the DDLS correlation function consists of up to five exponentials. The amplitude factors are a function of the elements of the polarizability tensor α and the rotational diffusion tensor Θ. For symmetric top molecules, however, α_{zz} ($\equiv\alpha_\parallel$) > α_{yy} = α_{xx} ($\equiv\alpha_\perp$), and the correlation function corresponding to eq 3 reduces to a one-exponential form given by

$$S^{VH}(q,t) = AN\beta^2(1 + fN) \exp-\left[\frac{t}{\tau_s}\left(\frac{1 + gN}{1 + fN}\right)\right] \tag{4}$$

where β ($=\alpha_\parallel - \alpha_\perp$) is the optical anisotropy of a molecule, A is a constant, N is the number of molecules, τ_s is the reorientational correlation time for a single molecule, and f and g are, respectively, the static and dynamic correlation factors. In general, $S^{VH}(q,t)$ includes information about dynamic correlations in orientation and position between all pairs of molecules through the static and dynamic correlation factors f and g. It has been found for many symmetric top molecules that the dynamic correlation factor $gN \ll 1$. Equation 4 is valid to a high degree of approximation for molecules that are almost symmetric tops like the DNA fragments studied here.

DDLS experiments are performed in the frequency domain, and the spectrum of the scattered light is measured by Fabry-Perot interferometry. With use of the Wiener–Khintchin theorem the correlation function may be transformed into the corresponding spectrum

$$S^{VH}(\omega) = AN\beta^2(1 + fN)[\Gamma/(\Gamma^2 + \omega^2)] \tag{5}$$

with

$$\Gamma = \frac{1}{2\pi}\frac{1 + gN}{1 + fN}\frac{1}{\tau_s}$$

The spectrum consists of a single Lorentzian line with a half-width at half-height Γ which is related to the correlation time, τ_{1s}, measured in the light scattering experiment by

$$\tau_{1s} = (2\pi\Gamma)^{-1} = [(1 + fN)/(1 + gN)]\tau_s \tag{6}$$

In ideal dilute solutions the pair correlation factors are negligible ($g = f = 0$) and DDLS measures the single-particle reorientational correlation time τ_s. Otherwise, concentration dependence measurements allow one to estimate the influence of pair correlation effects. Because only the rotation of the symmetry axis contributes to the depolarized spectrum, the reorientational relaxation time τ_s is simply dependent on $\Theta_\perp$, the rotational diffusion coefficient for rotation about the short axes of the elongated molecule (equal to the rotational diffusion coefficient for rotation of the long axis)

$$\tau_s = 1/6\Theta_\perp \tag{7}$$

Note that in this dilute solution limit, the DDLS correlation function in eq 4 reduces to the form in eq 3 with $A_m = 0$ for $m = \pm1, \pm2$.

In contrast to DDLS, NMR cross-relaxation usually results from an incoherent process. Relaxation between two protons is caused by the rapid fluctuations in the dipolar interaction due to random molecular reorientation. The process can be described (Spiess, 1978; Abragam, 1978) by the correlation functions as given in eq 2. Relaxation rates are commonly and conveniently expressed in terms of spectral densities, which are, as in the DDLS case, the Fourier transforms of the correlation functions

$$J(\omega) = \int_{-\infty}^{\infty} C^{NMR}(t)e^{-i\omega t}\,dt \tag{8}$$

The cross-relaxation rate between two protons in terms of the spectral densities is given by

$$\sigma_{ij} = (\gamma_H{}^4h^2/10r^6)[6J(\omega_i + \omega_j) - J(\omega_i - \omega_j)] \quad (9)$$

In the above equation, γ_H is the proton gyromagnetic ratio and ω_i and ω_j are the resonance frequencies of the two protons, which can be set equal to the frequency of the spectrometer.

While in DDLS only the rotation around an axis perpendicular to the symmetry axis of the cylinder causes a significant change in the polarizability tensor, the NMR correlation time is determined by the reorientation about the different axes. Woessner has shown that for axially symmetric molecules the effective correlation function may be calculated directly from the two rotational diffusion coefficients $\Theta_\perp$ and $\Theta_\parallel$. The form for the correlation function becomes

$$C^{NMR}(t) = \sum_{n=-2}^{+2} A_n \exp-\{[6\Theta_\perp + n^2(\Theta_\parallel - \Theta_\perp)]t\} \quad (10)$$

with the amplitude factors

$$A_0 = \tfrac{1}{4}(3\cos^2\theta - 1)^2$$

$$A_{\pm1} = \tfrac{3}{2}\cos^2\theta(1 - \cos^2\theta)$$

$$A_{\pm2} = \tfrac{3}{8}(\cos^2\theta - 1)^2$$

where θ is defined as the angle between the internuclear vector μ and the symmetry axis of the molecule. Note that this is of the same form as eq 3. Woessner used the rotational diffusion theory of Perrin (Perrin, 1934, 1936; Koenig, 1975) for ellipsoids. His formalism is also applicable to rigid rods (cylinders), which are often better models for the hydrodynamic properties of short DNA fragments. Several approximations can be applied to simplify the expression for σ to determine the effective correlation time from a cross-relaxation experiment. For large molecules where $\omega\tau \geq 1$, the term $J(\omega_i - \omega_j) \gg J(\omega_i + \omega_j)$, and so the $J(\omega_i + \omega_j)$ term in the cross-relaxation rate can be neglected. In addition, for the case of two protons, $\omega_i \approx \omega_j$, and so $J(\omega_i - \omega_j) = J(0)$. In this case, as may be seen from eq 8, $J(0)$ becomes the area under the correlation function that we define as the experimental rotation correlation time, τ_{nmr}. The final expression for the cross-relaxation rate becomes

$$\sigma_{ij} = (\gamma_H{}^4h^2/10r^6)\tau_{nmr} \quad (11)$$

For rotation of a rigid cylinder the correlation time τ_{nmr} can be calculated by using eq 10

$$\tau_{rb} = A_0(6\Theta_\perp)^{-1} + A_1(\Theta_\parallel + 5\Theta_\perp)^{-1} + A_2(4\Theta_\parallel + 2\Theta_\perp)^{-1} \quad (12)$$

where we have used the notation τ_{rb} (rb = rigid body) to indicate τ_{nmr} for this special case.

The DDLS spectrum depends on the rotational diffusion coefficient for rotation around the axes perpendicular to the symmetry axis ($\Theta_\perp$), while the NMR cross-relaxation rate depends on the rotational diffusion coefficients for rotation around both the symmetry axis and the axes perpendicular to it. These quantities are related to the length L and diameter d of the cylinder by hydrodynamic theories. Tirado and Garcia de la Torre evaluated the rotational friction and diffusion coefficients for cylinders with a small ratio of $p = L/d$. The rotational diffusion coefficient for the rotation of the symmetry axis is given by

$$\Theta_\perp = (3kT/\pi\eta_0L^3)(\ln p + \delta_\perp) \quad (13)$$

where η_0 is the solvent viscosity and k the Boltzmann constant. $\delta_\perp$ is the end-effect correction term, which is a function of p^{-1}

$$\delta_\perp = -0.662 + (0.917/p) - (0.050/p^2) \quad (14)$$

For rotation around the symmetry axis the diffusion coefficient is given by

$$\Theta_\parallel = kT/[A\pi\eta_0LR^2(1 + \delta_\parallel)] \quad (15)$$

where $A = 3.841$, R is the radius of the cylinder ($=d/2$), and $\delta_\parallel$ is also a function of p^{-1}

$$\delta_\parallel = 1.119 \times 10^{-4} + (0.6884/p) - (0.2019/p^2) \quad (16)$$

Tirado and Garcia de la Torre specified the region of validity of their interpolation equations for the end-effect terms as approximately $2 \leq p \lesssim 30$. This is merely the range for which their computations have been done. It is possible that the equations are good approximations for $p \leq 2$ (see below).

There exist at least five other approaches, empirical, theoretical, or both combined, that give expressions for $\Theta_\perp$ of rigid rods similar to eq 13. A comparison is given by Elias and Eden (1981). Each theory results in a different function for the end-effect terms. The Broersma (Broersma, 1960a,b; 1980) relation is valid only for large p, while the theories of Yoshizaki and Yamakawa (1980) and Mandelkern and Crothers (Elias & Eden, 1981) are supposed to be accurate for axial ratios down to $p \approx 5$. Neither of these last two approaches is applicable to molecules with axial ratios smaller than 3. Yoshizaki and Yamakawa have evaluated the transport coefficients for spherocylinders (cylinders capped with hemispheres). At very small values of p the influence of the end caps on the end-effect term δ becomes dominant. An extrapolation to zero cap size is not possible. On the other hand, the expression for $\delta_\perp$ from the Mandelkern and Crothers theory contains a quadratic term that gives physically unreasonable results for $p < 2.8$. Therefore, these alternative approaches were not considered to be appropriate for the small axial ratio DNA fragments studied here.

It should be emphasized that the theory presented in this section applies to rigid, cylindrically symmetric molecules. It does not include any possible effects from intramolecular motions. While it is thought that local, rapid intramolecular motions would not have important effects on the DDLS spectrum, such motions might make important contributions to the NMR cross-relaxation rates. Some effects of such motions are discussed below for various models in connection with our experimental results.

Materials and Methods

Oligonucleotides. The oligonucleotides $d(CG)_4$ and $d(CG)_6$ were purchased from Operon Technologies, Inc. (San Pablo, CA). The purity was verified by HPLC to be >98%. The DNA fragment d(CGCGTTGTTCGCG) was synthesized by the phosphoramidite method. Details about the preparation are given elsewhere (Williamson, 1988). The experiments were performed in a phosphate buffer (50 mM sodium phosphate, 100 mM NaCl, 2 mM EDTA, and 0.1% NaN_3) at pH 7.0 (for H_2O).

DDLS Experiments. A depolarized dynamic light scattering apparatus similar to one whose detailed description is given elsewhere (Eimer, 1987) was used. The light source was an argon ion laser (Spectra-Physics, Model 2000) operating in single mode at $\lambda = 488.0$ nm. The scattered light was collected at a scattering angle of 90° in the VH geometry and frequency analyzed by a piezoelectrically driven Fabry-Perot interferometer (RC-110, Burleigh Instruments). A set of 750-MHz confocal mirrors was used to allow the analysis of slow relaxation processes on the order of nanoseconds. The typical

finesse was about 80–90. The detection system consists of a photomultiplier tube (EMI, Model 9865), an amplifier discriminator (SSR 1105), and a data acquisition and stabilization unit (DAS-1, Burleigh Instruments). Because of the low intensity of the depolarized scattered light, at the beginning of each scan a small portion of diffuse, unscattered light (incidence angle = 180°) was passed through the interferometer for stabilization purposes. Thereafter, 2 orders of scattered light were collected. The measuring and reference beam are controlled by a shutter system (Newport, Model 845). Data analysis was performed on a microcomputer (Universe 68, Charles River Data System). All spectra were deconvoluted by using an iterative method (van Cittert, 1931), using the spectrum of the unscattered light mentioned above as the instrumental function. In some cases, due to the influence of dust, the spectrum of the depolarized light contained a narrow line with a half-width at half-height equal to that of the instrument. Nevertheless, a deconvolution with two Lorentzians gave the reorientational correlation time of the oligonucleotides. The amplitude of the narrow component was less than 10%.

NMR Experiments. All measurements were performed on a GE GN-500 spectrometer at 500 MHz. NMR samples were prepared by lyophilization of a known amount of oligonucleotide from H_2O, the appropriate buffer solutions were added, and the sample was exchanged for D_2O by repeated lyophilization from 99.8% D_2O. The samples were finally dissolved in the original volume of 99.996% D_2O in a glovebag under nitrogen. The samples of $d(CG)_4$ and $d(CG)_6$ contained 50 mM sodium phosphate, pH 7.0, 100 mM NaCl, and 2 mM EDTA. The sample of d(CGCGTTGTTCGCG) contained 35 mM sodium phosphate, pH 7.0, 70 mM NaCl, and 5 mM EDTA.

Cross-relaxation rates were determined by measuring the time dependence of the NOE. Five spectra were recorded in an interleaved fashion, one as a control with no irradiation and four with selective saturation of one resonance with incremental irradiation times. The irradiation times were chosen, depending upon the oligonucleotide and temperature, such that the magnitude of the largest NOE in a series was <20%. NOEs were quantitated by subtracting spectra with and without NOE and then integrating the peak areas in the difference spectra. Cross-relaxation rates were obtained from the slope of the least-squares line through the NOE vs time data. The effective correlation times reported were calculated from the measured σ by using a value for $r_{(H5-H6)}$ of 2.47 Å.

Results and Discussion

Depolarized Dynamic Light Scattering. The measured orientational correlation time in DDLS is determined by the rotation of the oligonucleotides around their minor axes. To assure that under our experimental conditions the pair correlation factors do not play a significant role, depolarized spectra of the three synthetic oligonucleotides $d(CG)_4$, $d(CG)_6$, and d(CGCGTTGTTCGCG) were taken at different concentrations. Within the range from 2 to about 8 mg/mL no concentration dependence of τ_{1s} is observed. The DDLS correlation time of the dodecamer sample with the highest concentration studied (12 mg/mL) is within experimental error the same as that found for the lower concentrations. Only the highest measured concentration (15.7 mg/mL) of the octamer indicates a slight but significantly larger correlation time. Otherwise, concentration effects are negligible below 8 mg/mL, and therefore DDLS gives directly the single particle relaxation time. These results are in agreement with recent steady-state fluorescence polarization studies (Hård & Kearns, 1986) on the aggregation of DNA fragments with a length of 30–90 base pairs.

The values of τ_{1s} of the different DNA fragments vary between about 2 ns for the tridecamer and 6.5 ns for the dodecamer at 20 °C. This is a relatively large and easily measured variation. The $d(CG)_6$ dodecamer has the longest correlation time with 6.3 ns. The relaxation time of the four bases shorter octamer is about 50% faster. It is known that both oligonucleotides form a double helix of the B-DNA type under the experimental conditions. The tridecamer, on the other hand, exists in a hairpin structure. The d(CG) regions at both ends are self-complementary and form an intramolecular double helix (the stem region). The five unpaired bases in the center of the molecule form the loop region with some kind of stacking interaction. This results in a nearly spherical shape of the oligonucleotide with a smaller size than the double-helical d(CG) oligomers. Therefore, the tridecamer exhibits the shortest correlation time (1.9 ns). These results show that by DDLS it is possible to distinguish between fragments which differ in length by four base pairs by DDLS measurements. The large difference in τ_{1s} for the octamer and dodecamer suggests that small changes in the length (for instance, those due to intercalation) can be monitored with high sensitivity by this method.

As outlined under Theory, it is possible to calculate the dimensions of the rodlike DNA fragments from the rotational correlation times by using the expressions of Tirado and Garcia de la Torre for the rotational diffusion coefficients $\Theta_\perp$ and $\Theta_\parallel$. The values for τ_{1s} of the octamer and dodecamer correspond to the reorientation of a cylinder with a diameter of 20.5 ± 1 Å and a length of n3.4 Å, where n is the number of bases per strand. This is significantly smaller than the value of 24–26 Å that is commonly used for the hydrodynamic diameter of B-DNA in the literature. The hydrodynamic diameters obtained from various experimental techniques generally range from 20 to 28 Å, on the basis of a rise per base pair of 3.4 Å. The DNA fragments studied by most of these methods are usually fairly long and, therefore, long-range bending and twisting modes complicate the analysis. Furthermore, with increasing length the relative change of the diffusion coefficients with the diameter of the cylinder is smaller. Photon correlation experiments (Eimer and Pecora, unpublished results) have been used to measure the translational diffusion coefficient of the octamer, the dodecamer, and a 20-mer. These results, when combined with the DDLS results reported here, and the Tirado and Garcia de la Torre relations yield values for the fragment diameter without making assumptions about either the rise per base pair or the fragment length. These results, which will be published elsewhere, further confirm the value obtained here for the hydrodynamic diameter of double-helical DNA. Assuming a spherical shape, the diameter of the hairpin molecule is calculated to be 24.5 ± 1.5 Å by using the Stokes–Einstein–Debye relation.

The experimental single-particle correlation times are related to the macroscopic viscosity of the solvent by the Stokes–Einstein–Debye (SED) equation (Dote & Kivelson, 1983)

$$\tau_s = V_h(\eta_0/kT) + \tau_0 \qquad (17)$$

with

$$V_h = f(p)z(p)V_m$$

The SED relation allows us to estimate the effective hydrodynamic volume V_h from the viscosity dependence of τ_s. The functions $f(p)$ and $z(p)$ are the form and hydrodynamic boundary condition factors that relate the hydrodynamic volume to the volume of the rotating species, V_m. Both factors

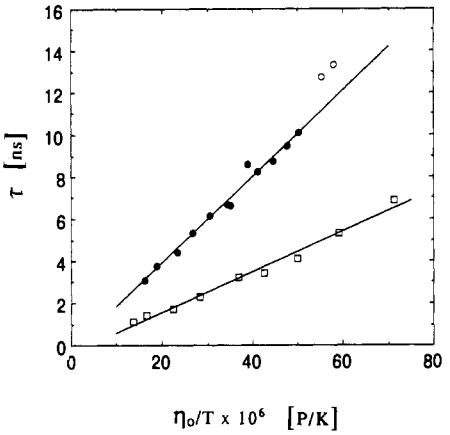

FIGURE 1: Stokes–Einstein–Debye plot of the relaxation data from the dodecamer $d(CG)_6$. (●), (○) DDLS correlation times τ_{1s} at different temperatures; (○) highlights the values at low temperature, which show a deviation from the SED behavior, due to aggregation. (□) NMR relaxation times τ_{nmr}, calculated from the cross-relaxation rates of the H5 and H6 protons of the inner cytidine residues 5, 7, and 9 (see Table I). The concentration of the oligonucleotide in both experiments is the same (12 mg/mL).

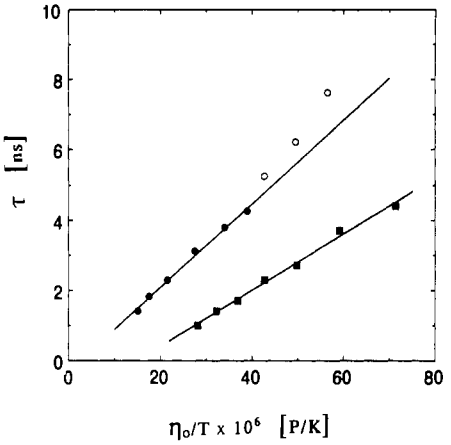

FIGURE 2: Stokes–Einstein–Debye plot of the relaxation data from the octamer $d(CG)_4$. (●), (○) DDLS correlation times τ_{1s} at different temperatures; (○) highlights the values at low temperature, which show a deviation from the SED behavior, due to aggregation. (■) NMR relaxation times τ_{nmr}, calculated from the cross-relaxation rates of the H5 and H6 protons of the cytidine residue 5 (see Table I). The concentration of the oligonucleotide in both experiments is the same (15.7 mg/mL).

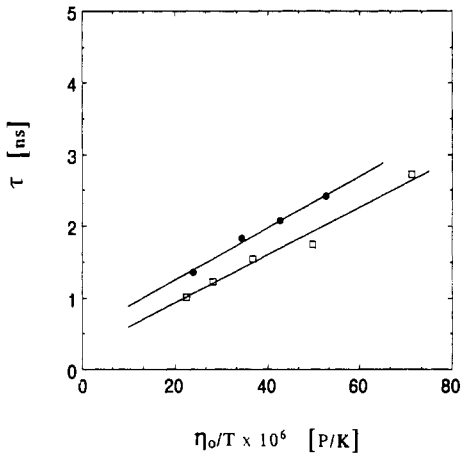

FIGURE 3: Stokes–Einstein–Debye plot of the relaxation data from the tridecamer d(CGCGTTGTTCGCG). (●) DDLS correlation times τ_{1s} at different temperatures; values are taken from both concentrations. (□) NMR correlation times τ_{nmr} from Williamson and Boxer (1989).

are functions of the shape parameters p. They can be calculated for molecules of a number of different shapes. For a sphere under stick boundary conditions (the first solvent layer experiences the same force as the surface of the solute molecule) $f(p) = 1$ and $z(p) = 1$. Therefore, the slope in an SED plot should give immediately the volume of the rotating molecule. In case of slip boundary conditions (no angular momentum transfer between solute molecule and the solvent layer) $z(p) = 0$. Thus, in the slip case the correlation time is independent of the solvent viscosity for spheres. Perrin calculated the shape factor $f(p)$ for a biaxial ellipsoid under stick conditions. Youngren and Acrivos (1976) later generalized this result to triaxial ellipsoids. The corresponding shape factor for a cylinder may be evaluated from the recent calculations of the rotational friction coefficients by Tirado and Garcia de la Torre. Hydrodynamic slip conditions are considered by Hu and Zwanzig (1974) for a biaxial ellipsoid and are also included in the work of Youngren and Acrivos. Whether the rotational diffusion process occurs under slip or stick conditions depends mostly on the relative size of the solvent and solute molecules and the interaction forces. A detailed discussion is given by Kivelson (1987).

Figures 1–3 illustrate the dependence of the reorientational correlation time τ_{1s} from DDLS on η_0/T for the three DNA fragments. The change in η_0/T was achieved by measuring the temperature dependence of τ_{1s} of the most concentrated solutions of the d(CG) octamer (15.7 mg/mL) and the dodecamer (12.0 mg/mL). The temperature was varied between 2 and 60 °C. For the hairpin molecule relaxation times from both concentrations were considered. The viscosity η_0 is assumed to be that of H_2O and was taken from the literature (*CRC Handbook*, 1980). The effect of the added buffer on the viscosity is estimated to be less than 3% and was neglected.

The correlation times of the dodecamer obtained from DDLS show a linear dependence on η_0/T above 7 °C. Below that temperature a significant deviation to longer relaxation times is observed, which indicates that at low temperature $d(CG)_6$ tends to aggregate to some extent. The octamer exhibits the same effect, though the nonlinear behavior appears at higher temperature (about 20 °C). This is reasonable because the octamer was studied at higher concentration than the dodecamer, and therefore the aggregation should persist at a higher temperature. The results from concentration-dependent measurements of $d(CG)_4$ support the idea of aggregation at about 20 °C. On the other hand, the SED plot of the hairpin molecule is well described by a straight line for both concentrations over the whole concentration range.

For all three oligonucleotides the hydrodynamic volume is calculated from the linear regions in the SED plots. Table I displays the effective hydrodynamic volume obtained from the experimental correlation times and the calculated values under stick boundary conditions. The shape factor $f(p)$ for the octamer and dodecamer is calculated by using the Tirado and Garcia de la Torre theory for a rodlike molecule. It is defined as the ratio of the relaxation times of a cylinder to that of a sphere with the same volume.

$$f(p) = \tau_{cyl}/\tau_{sp} = \tfrac{2}{9}p^2(\ln p + \delta_\perp)^{-1} \qquad (18)$$

For comparison, the diameter of the cylinder was varied from 20 to 24 Å. In the case of the hairpin molecule the hydrodynamic volume is compared to the volume of a sphere with a diameter between 20 and 23 Å.

For the rodlike DNA fragments $d(CG)_6$ and $d(CG)_4$ the experimental hydrodynamic volume corresponds to a cylinder with a diameter of 21.5 and 22.5 Å. This is a slightly larger

Table I: Comparison of the Experimental Hydrodynamic Volumes V_h from DDLS and NMR with Theoretical Values Calculated According to Equation 17 under Hydrodynamic Stick Conditions[a]

(a) $d(CG)_6$

		DDLS		NMR	
d (Å)	V_{cyl}	V_h^{theo} $(=V_m f^{\perp})$	V_h^{exp}	V_h^{theo} $(=V_m f^{\parallel} S^2)$	V_h^{exp}
20	12820	24270		10650	
21	14480	26870		11940	
22	16270	29640	28400 ± 2200	13330	13600 ± 1100
23	18200	32600		14800	
24	20270	35750		16410	

(b) $d(CG)_4$

		DDLS		NMR	
d (Å)	V_{cyl}	V_h^{theo} $(=V_m f^{\perp})$	V_h^{exp}	V_h^{theo} $(=V_m f^{\parallel} S^2)$	V_h^{exp}
20	8550	12000		6400	
21	9700	13590		7300	
22	11100	15320		8740	
23	12550	17190	16450 ± 1500	9330	
24	14110	19200		10500	10000 ± 1000

(c) d(CGCGTTGTTCGCG)

		DDLS	NMR
d (Å)	V_{sph}	V_h^{exp}	V_h^{exp}
20	4190		
21	4850		4650 ± 500
22	5580	5050 ± 500	
23	6370		

[a] V_m is the volume of a cylinder whose dimensions are defined by the length of the oligonucleotides (based on a rise per base of 3.4 Å) and a diameter of 20.5 Å. The shape factors are calculated by using the Tirado and Garcia de la Torre theory. The volumes are given in cubic angstroms.

diameter than estimated from the concentration-dependent measurements of τ_{1s} at 20 °C. But taking into account an error of ±10% for the slope in the SED plots, the agreement is very good. The hydrodynamic value of the hairpin molecule fits to that of a sphere with a diameter of 21.5 ± 2.0 Å. At this point it should be mentioned that besides the difference in the absolute correlation times, the hairpin and the double-helical structures can also be easily distinguished by the effective hydrodynamic volume. Furthermore, the rotational motion of the DNA fragments is very well described by hydrodynamic stick boundary conditions. This is expected because the oligonucleotides are large in size in comparison to the solvent molecules.

Figure 4 shows the relaxation times of the octamer and dodecamer plotted versus $[(\eta_0/T)L^3](\ln p + \delta_\perp)^{-1}$ according to eq 13. The values of $\delta_\perp$ are calculated from the theory of Tirado and Garcia de la Torre by using $p = 1.35$ (octamer) and 2.01 (dodecamer). Except for the low-temperature values (open symbols) both data sets fall on a single straight line. As mentioned above, the range of validity of eq 14 and 16 is estimated by Tirado and Garcia de la Torre to be $2 \leq p \lesssim 30$. They estimate the lower limit to be $p = 2$ because the data from which their equations were obtained were limited to values of p between 2 and 20. Our data show that the rotational motion of a set of cylindrically symmetric molecules with p as low as 1.35 is well described by the theory of Tirado and Garcia de la Torre.

NMR Cross-Relaxation. The cross-relaxation rates σ between the H5 and H6 protons of the cytosine residues were determined by measuring the magnitude of the NOE for different irradiation times. According to eq 11 the rotational correlation time τ_{nmr} is directly related to σ. The T_1 relaxation time of the thymidine C6 carbons of the hairpin molecule from a ^{13}C-enriched sample was also measured. The correlation times from carbon relaxation and H5–H6 cross-relaxation were the same within experimental error. The resulting experimentally determined τ_{nmr} values of the different thymidine (Williamson & Boxer, 1989) and cytosine residues are summarized in Table II.

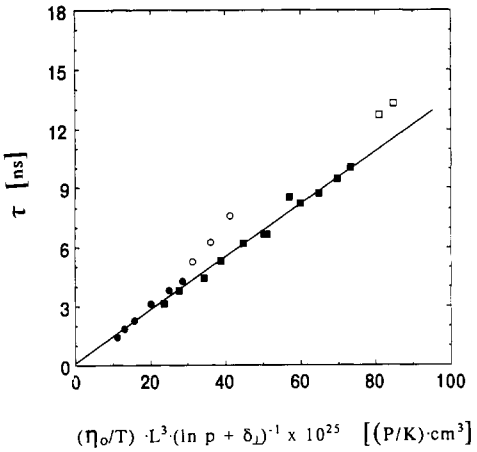

FIGURE 4: DDLS correlation times τ_{1s} from $d(CG)_4$ and $d(CH)_6$ as a function of $[(\eta_0/T)L^3](\ln p + \delta_\perp)^{-1}$ according to the Tirado and Garcia de la Torre theory; (●), (○) $d(CG)_4$, (■), (□) $d(CG)_6$. d = 20.5 Å, which yields $p = 1.35$ [$d(CG)_4$] and $p = 2.01$ [$d(CG)_6$]. $\delta_\perp$ is calculated from eq 14.

Table II: Rotational Correlation Times of the Oligonucleotides Calculated from the Cross-Relaxation Rates between Cytosine H5 and H6 in Nanoseconds (See Equation 11)

(a) $d(CG)_6$

temp (°C)	Cy (11)	Cy (3)	Cy (5,7,9)
5	6.7	7.0	6.9
10	4.7	5.1	5.3
15	3.9	4.0	4.1
20	3.0	3.1	3.4
25	2.9	2.9	3.2
48	1.3	1.5	1.7
35	1.9	1.9	2.3
60	1.1	1.2	1.4
70	0.83	0.84	1.1

(b) $d(CG)_4$

temp (°C)	Cy (3)	Cy (5)	Cy (7)
5	4.1	4.4	3.4
10	3.4	3.7	3.2
15	2.6	2.7	2.3
20	2.0	2.3	1.9
25	1.76	1.7	1.8
35	1.2	1.4	1.4
48	0.86	1.0	1.0

(c) d(CGCGTTGTTCGCG)[a]

temp (°C)	T (5,6,8,9)	temp (°C)	T (5,6,8,9)
5	2.8	35	1.2
15	1.7	45	1.0
25	1.5		

[a] Calculated from T_1 and NOE measurements on the thymidine C6 carbon [see Williamson and Boxer (1989)].

For the dodecamer the central cytosines show slightly longer correlation times than the Cy (3) and Cy (11). This effect becomes more significant at higher temperatures. This indicates that there is more flexibility at the outer ends of the double helix than near the center. As expected, the fraying increases with increasing temperature. The H5 signal from Cy (1) could not be resolved from the sugar proton resonances and was not quantitated. The correlation times τ_{nmr} of the different cytosine residues in the octamer are the same within experimental error.

The NMR relaxation times for the three oligonucleotides were studied at various temperatures from 5 to 65 °C. The dependence of τ_{nmr} on η_0/T is shown in Figures 1–3 together

with the DDLS data. For η_0 the viscosity of pure D_2O (Millero et al., 1971) was used and, as in the case of the DDLS experiments, the relatively small effects of the buffer and salt were neglected.

The correlation times τ_{nmr} of the three DNA fragments studied vary linearly with η_0/T. For the dodecamer the slope of the best-fit straight line is significantly smaller than that from the SED plot of the DDLS data. The same effect can be observed for the octamer, though the difference in the slopes is smaller. In the case of the hairpin molecule the temperature dependence of the rotational correlation times from NMR and DDLS gives the same slope and therefore results in the same hydrodynamic volume. This is a confirmation of the fact that the tridecamer assumes a nearly spherical shape and both the DDLS and NMR methods should monitor the same rotational motion.

For asymmetric molecules these techniques measure a differently weighted combination of the reorientational relaxation times about the different molecular axes. Therefore, different effective hydrodynamic volumes should be obtained from the slopes of the SED plots. With increasing axial ratio p the discrepancy in the shape factor and thereby the difference in V_h becomes more distinct. This effect is illustrated in the experimental hydrodynamic volumes from NMR and DDLS shown in Table I. With increasing asymmetry from the octamer to the dodecamer the gap between the V_h values increases.

Analogous to the DDLS results, we assume that the SED equation (see eq 17) can be used to describe the viscosity dependence of the rotational relaxation time as measured by the NMR experiment. As discussed in detail below, the experimental correlation time τ_{nmr} appears to be considerably influenced by internal motions and can be approximated by eq 27. This yields

$$S^2\tau_{rb} + (1 - S^2)\tau_{int} = V_h(\eta_0/kT) + \tau_0 \qquad (19)$$

where τ_{rb} is the overall correlation time, calculated for a rigid cylinder according to eq 12, τ_{int} is the relaxation time due to any rapid intramolecular librational motion that may be occurring, and S is the order parameter discussed below. Note that the hydrodynamic volume is not the same as that measured by DDLS, both because of the anisotropy effect discussed above and because the order parameter for the internal motion reduces τ_{rb} by the factor S^2. Any significant dependence of τ_{int} on the solvent viscosity would result in a nonlinear SED plot. The characteristics of any librational motion should be determined mainly by internal constraints imposed by the secondary helical structure of the oligonucleotides. Though parts of the bases are exposed to the solvent, friction effects from the solvent molecules are expected to play a minor role. For the small oligonucleotides studied here, the term $(1 - S^2)\tau_{int}$ is negligible and therefore

$$S^2\tau_{rb} = V_m f''(p)S^2(\eta_0/kT) + \tau_0 \qquad (20)$$

The corresponding shape factor $f''(p) = \tau_{rb}/\tau_{sphere}$ is calculated by using eq 12, and hence it is possible to estimate the hydrodynamic volume expected for the NMR data. The calculated hydrodynamic volumes [$V_h = V_m f''(p)S^2$] are listed in Table I for various diameters of the different cylinders as mentioned before. The experimental hydrodynamic volume of the dodecamer corresponds to a diameter of about 22 Å, while the octamer data are consistent with a slightly larger diameter of 23.5 Å. Within the experimental error, which is estimated to be ±2 Å for the NMR experiments, the agreement for the dimensions of the rodlike DNA fragments with results obtained from DDLS is very good.

Table III: Rotational Correlation Times of the DNA Fragments from DDLS and NMR Relaxation Measurements (T = 20 °C)

	τ_{ls} (ns)	τ_{nmr} (ns)
d(CGCGTTGTTCGCG)	1.9 ± 0.2	1.4 ± 0.3[a]
$d(CG)_4$	3.2 ± 0.2	1.55 ± 0.3
$d(CG)_6$	6.35 ± 0.3	2.95 ± 0.4
d(ATATCGATAT)		2.5 ± 0.4[b]
$d((CG)_3(TA)_2(CG)_3)$		4.2 ± 0.4[b]
20-mer		5.75 ± 0.5[c]

[a] Williamson and Boxer (1989). [b] Ikuta et al. (1986). [c] Lane et al. (1986).

In contrast to the DDLS results, the NMR data for the octamer and dodecamer exhibit no deviation from linear dependence of τ_{nmr} on η_0/T in the SED plots at low temperatures. This might be explained by the different sensitivities of these methods with respect to aggregation. The NMR resonance signal is proportional to the number density of the corresponding species. As may be seen from eq 5, the square of the optical anisotropy β of the scattering molecule determines the DDLS scattering intensity. Assuming an end-to-end stacking of double-helical $d(CG)_n$ molecules in an aggregate, the optical anisotropy of the aggregates should vary as the aggregation number times the optical anisotropy of the monomer. Due to the square law dependence of S^{VH} on β^2 (eq 5), the aggregates contribute overproportionally to the scattering intensity. Furthermore, because DDLS is a coherent process, any kind of parallel orientation of two double-helical molecules should influence the static pair correlation factor and therefore increase the apparent correlation time τ_{ls}.

Comparison of DDLS and NMR Results. As outlined under Theory, DDLS measures the end-over-end rotational correlation time. In NMR cross-relaxation experiments, the reorientation around both the symmetry axis of the cylinder and the axes perpendicular to it, as well as any internal motion of the internuclear vector, contributes to the experimental effective correlation time τ_{nmr}.

The experimental correlation times τ_{ls} and τ_{nmr} at 20 °C of the different DNA fragments are compared in Table III. The NMR data are corrected for the difference in viscosity between H_2O and D_2O. In both data sets the reorientational relaxation times are correlated to the length and conformation of the DNA fragments, though the effect is more distinct for the DDLS results. The observed τ_{nmr} values are always substantially smaller, and the difference from τ_{ls} increases with increasing length of the oligonucleotides. For the hairpin molecule with nearly spherical shape, the correlation times from both methods come very close.

As discussed previously, a combination of the recent calculations of Tirado and Garcia de la Torre of the rotational diffusion coefficients $\Theta_\perp$ and $\Theta_\parallel$ for cylindrically symmetric molecules of short axial ratios and Woessner's theory according to eq 12 makes it possible to calculate the effective correlation time τ_{rb} as measured by NMR.

A comparison of the experimental data with theoretical values is given in Figure 5. The results obtained from DDLS fit very well to calculated values for a cylinder with a diameter of 20.5 Å and a length of n3.4 Å, where n is the number of base pairs per strand. The measured rotational relaxation time of a 43-mer by transient electric birefringence (Wu et al., 1987) is also consistent with these model assumptions. To clarify the sensitivity of the correlation times to any change in size and shape, the theoretical values for DNA fragments with the same rise per base but different diameters of 19 and 22 Å are also shown. Figure 5 illustrates that for short cylinders the theoretical correlation times $\tau_\perp$ ($=1/6\Theta_\perp$) and τ_{rb}

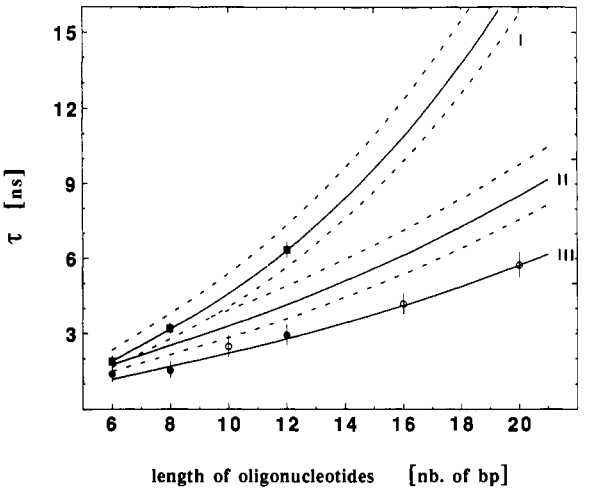

FIGURE 5: Comparison of experimental with theoretical rotational correlation times for oligonucleotides of various lengths. (■) Experimental DDLS correlation times τ_{1s} from $d(CG)_4$, $d(CG)_6$, and the tridecamer d(CGCGTTGTTCGCG); (●) corresponding NMR data. It is assumed that the correlation times of the tridecamer, which forms a spherical hairpin structure, are comparable to that of a double-helical hexamer. (○) Experimental NMR correlation times from a decamer [d(ATATCGATAT)], a hexadecamer $[d(CG)_3(TA)_2(CG)_3]$ (Ikuta et al., 1986), and a 20-mer (Lane et al., 1986). (I) Theoretical correlation times for the rotation of the symmetry axis ($\tau_\perp = 1/6\Theta_\perp$) from the Tirado and Garcia de la Torre formulas (eq 13). (II) Corresponding values of τ_{nmr} from eq 12. Calculations are based on a rise per base of 3.4 Å, a diameter of 20.5 Å, $T = 20$ °C, and $\eta_0 = 1.002$ cP. The broken lines above are computed for $d = 22$ Å and below for $d = 19$ Å. (III) Theoretical effective correlation times, taking into account local internal motion, using the Lipari–Szabo formula (eq 27) with $S = 0.82$ and $\tau_{int} = 50$ ps. Assuming diffusion in a cone, the general order parameter corresponds to $\theta_0 = 29°$.

change significantly with the dimensions of the underlying model in comparison to the experimental errors of τ_{1s} and τ_{nmr} from the relaxation measurements. DDLS is especially sensitive to changes in the dimensions and shape of short oligonucleotides such as those studied here.

Tirado et al. (1984a) compared a number of experimental data sets of the rotational diffusion coefficients from DNA fragments with a length between 50 and 188 bases per strand. Assuming a rise per base of 3.4 Å, the hydrodynamic diameter varies between 20 and 28 Å. With increasing axial ratio $p = L/d$ of the cylinder, the relative change of the rotational correlation times with diameter decreases. For that reason it is possible to estimate the diameter of the DNA B-helix from a short fragment with a greater precision than from a longer fragment. For example, if one increases the diameter from 20 to 26 Å, the correlation time of the dodecamer would slow by about 40% compared to a 10% difference for a 150-mer. Besides, it is doubtful that the long oligonucleotides can be modeled as rigid rods, because it is likely that collective internal bending and twisting motions influence the overall tumbling correlation time. Our results for short oligomers indicate that the best estimate of the hydrodynamic diameter of DNA is 20.5 ± 1 Å.

A comparison of the experimental correlation times τ_{nmr} with the theoretical τ_{rb} shows that the τ_{nmr} are significantly faster than expected for a rigid rod with the dimensions obtained from the DDLS experiments. Besides our NMR data in Figure 5, results from a decamer [d(ATATCGATAT)], a hexadecamer $[d(CG)_3(TA)_2(CG)_3]$ (Ikuta et al., 1986), and a 20-mer (Lane et al., 1986) are also shown. All NMR correlation times were determined by NMR cross-relaxation experiments or semiselective spin–lattice relaxation. With increasing length of the DNA fragments, the deviation from τ_{rb} (see eq 12) becomes more substantial and is well beyond the experimental error. In general, the experimental correlation time is about 30% faster than τ_{rb} for all oligonucleotides studied. This result is best explained by the fact that the measured τ_{nmr} is not only determined by the overall reorientation of the molecules but also incorporates some internal motion.

Internal Mobility of the Bases. In the following we analyze the discrepancy in the observed correlation times from NMR and the calculated one for a rigid body, on the basis of the DDLS results. The difference can be explained by the librational motion of the bases within the double helix. The experimental data are analyzed in the light of three different dynamic models.

Lipari and Szabo (1982a,b) have proposed a model-free approach. It gives a simple expression for the combination of overall and internal motion that includes a so-called general order parameter S. This parameter reflects the degree of spatial restriction of the internal motion. The wobbling dynamics is assumed to be characterized by a single correlation time τ_{int} that is much faster than the overall correlation time. In the following we give a brief outline of the underlying ideas.

In general, the time correlation function for the dynamics of a cylindrically symmetric molecule that undergoes overall as well as local internal motion is given by

$$C(t) = \sum_{n=-2}^{+2}\sum_{c=-2}^{+2} \exp-\{[6\Theta_\perp + n^2(\Theta_\parallel - \Theta_\perp)]t\}[d_{nc}^{(2)}(\beta_{MD})]^2 C^i_c(t) \quad (21)$$

with the internal motion correlation function defined by

$$C^i_c(t) = \langle D^{(2)*}_{c,0}[\Omega_{MF}(0)] D^{(2)}_{c,0}[\Omega_{MF}(t)] \rangle \quad (22)$$

where $[d_{nc}^{(2)}(\beta_{MD})]^2$ are the reduced Wigner rotation matrix elements (Brink & Satchler, 1968). The angles Ω_{MF} in the internal correlation function $C^i_c(t)$ describe the orientation of μ relative to a director D, which forms a fixed angle β_{MD} with the symmetry axis of the cylinder. For a rigid molecule $C^i_c(t) = \delta_{c,0}$, and eq 21 reduces to the Woessner expression given in eq 10; the remaining $[d_{n0}^{(2)}(\beta_{MD})]^2$ correspond to the amplitude factors in eq 12. Numerical calculations (Lipari & Szabo, 1982a) have shown that the total correlation function can, without large errors, often be factored into a product of contributions due to overall and internal motion

$$C(t) = C^o(t) C^i(t) \quad (23)$$

with

$$C^o(t) = \sum_{n=-2}^{+2} \exp-\{[6\Theta_\perp + n^2(\Theta_\parallel - \Theta_\perp)]t\}[d_{n0}^{(2)}(\beta_{MD})]^2$$

It must be emphasized that this is an approximation which has been shown to be valid when the rate constant for the internal motion is much faster than that characterizing the overall reorientation. Furthermore, the internal motion has to be in the extreme narrowing limit, $(\omega\tau_{int})^2 \ll 1$.

If the internal motion is diffusive or jumplike, $C^i(t)$ can be expressed as a series of exponentials

$$C^i(t) = \sum_{i=0} A_i \exp-(t/\tau_i) \quad (24)$$

The simplest approximation to $C^i(t)$ that is exact at $t = 0$ and $t = \infty$ is given by

$$C^i(t) = S^2 + (1 - S^2) \exp-(t/\tau_{int}) \quad (25)$$

where S is the generalized order parameter which is, as mentioned before, a model-independent measure of the spatial

restriction of the internal motion. It can be expressed as an equilibrium average and contains no information about the time scale of the internal dynamics. The effective correlation time τ_{int} is related to the microscopic rate constant and spatial nature of the motion. τ_{int} can be characterized only within a certain dynamic model. According to eqs 12, 23, and 25 the total correlation function is given by

$$C(t) = S^2 \exp-(t/\tau_{rb}) + (1 - S^2) \exp-(t/\tau) \quad (26)$$

with

$$\tau^{-1} = \tau_{rb}^{-1} + \tau_{int}^{-1}$$

τ_{rb} is the effective overall correlation time for a rigid rod which is determined by $\Theta_\perp$ and $\Theta_\parallel$ and the orientation of the internuclear vector according to eq 12. If as assumed above the overall reorientation is much slower than the internal motion and τ_{int} is in the extreme narrowing limit, the measured correlation time in the NMR experiment can be approximated by

$$\tau_{nmr} = S^2\tau_{rb} + (1 - S^2)\tau_{int} \quad (27)$$

The available NMR data have been analyzed according to eq 27. The effective overall correlation time was calculated from eq 12 by using the dimensions of the rodlike oligomers from DDLS measurements. S was set to 0.82 and τ_{int} to 50 ps. To verify the validity of the approximations made in eq 27, we also calculated τ_{nmr} from eq 21 for the diffusion in a cone model (see below). The internal correlation function was calculated according to the method of Lipari and Szabo (1981)

$$C^i_c(t) = C_c(\infty) + [C_c(0) - C_c(\infty)] \exp(-t/\tau_{int}) \quad (28)$$

which gives formally the same expression as the model-free approach in eq 25. $C_c(\infty)$ and $C_c(0)$ are given in Lipari and Szabo (1981). For $\tau_{int} < 100$ ps and a tilt angle $\leq 20°$, the correlation times from eqs 21 and 27 differ by less than 2%. The error increases to about 3% when an internal correlation time of 200 ps is assumed. The overall rotational relaxation times used in these calculations were typical for the molecules studied. Furthermore, the theoretical calculations clearly indicate that the effect of the internal correlation time τ_{int} on τ_{nmr} in eq 27 is small compared to that of the order parameter S. Therefore, it is not possible to characterize the time constant of the librational motion precisely.

As can be seen from Figure 5 all NMR relaxation times of the different DNA fragments can be very well described by the model-free approach. It appears that the NMR cross-relaxation rate is significantly affected by the internal motion of the bases. The relaxation data are obtained from a number of oligonucleotides with very different base sequences. Figure 5 illustrates that within the experimental error the amplitude of the internal dynamics is independent of the length and base composition of the DNA fragments.

Up to this point the nature of the local internal motion has not been characterized, except for the assumption that it is a single-exponential decay to some base-line value. The parameters S^2 and τ_{int} have no special physical implication. The next step is to find one or more dynamic models, which might describe the observed motion in a meaningful way, and to evaluate the time correlation function. For the diffusion in the cone model, where the internuclear vector μ forms an angle β with the symmetry axis of the molecule and diffuses in a cone of semiangle θ_0, the internal correlation function $C^i(t)$ in eq 21 is known. Again it is assumed that the local internal motion decays much faster than the overall reorientation and therefore the asymptotic value of $C^i_c(\infty)$ contributes as an amplitude factor to the total correlation function. It was shown by Wang and Pecora (1980) that only $C^i_0(\infty)$ has a nonzero value which is given by

$$C^i_0(\infty) = [\tfrac{1}{2} \cos \theta_0(1 + \cos \theta_0)]^2 \quad (29)$$

and which is related to the order parameter for diffusion in a cone (see eq 27)

$$S_{cone} = \tfrac{1}{2} \cos \theta_0(1 + \cos \theta_0) = [C^i_0(\infty)]^{1/2} \quad (30)$$

The value of the generalized order parameter obtained by our fits to the oligonucleotide data, $S = 0.82$, corresponds to a cone angle of 29°.

A different approach is to assume that the intermolecular vector between the two protons undergoes overdamped librations about the equilibrium position in harmonic polar and azimuthal potential wells. The internal correlation functions are given by (Schurr & Fujimoto, 1988; Schurr, 1984)

$$C^i_0(t) = \tfrac{1}{4}\{\tfrac{1}{4} + \tfrac{3}{2} \cos(2\epsilon_0) \exp[-2\langle\delta\epsilon^2\rangle] + \tfrac{9}{8} \cos(4\epsilon_0) \exp[-4\langle\delta\epsilon^2\rangle(1 + \exp(-t/\tau_\epsilon))] + \tfrac{9}{8} \exp[-4\langle\delta\epsilon^2\rangle(1 - \exp(-t/\tau_\epsilon))]\} \quad (31a)$$

$$C^i_1(t) = \tfrac{3}{8}\{\exp[-4\langle\delta\epsilon^2\rangle(1 - \exp(-t/\tau_\epsilon))] - \cos(4\epsilon_0) \exp[-4\langle\delta\epsilon^2\rangle(1 + \exp(-t/\tau_\epsilon))]\} \exp[-\langle\delta\zeta^2\rangle(1 - \exp(-t/\tau_\zeta))] \quad (31b)$$

$$C^i_2(t) = \tfrac{3}{16}\{1 - 2 \cos(2\epsilon_0) \exp[-2\langle\delta\epsilon^2\rangle] + \tfrac{1}{2} \exp[-4\langle\delta\epsilon^2\rangle(1 - \exp(-t/\tau_\epsilon))] + \tfrac{1}{2} \cos(4\epsilon_0) \exp[-4\langle\delta\epsilon^2\rangle(1 + \exp(-t/\tau_\epsilon))] \exp[-4\langle\delta\zeta^2\rangle(1 - \exp(-t/\tau_\zeta))] \quad (31c)$$

where ϵ_0 ($=\beta$ in eq 21) is the angle between the internuclear vector and the symmetry axis of the cylinder and τ_ϵ and τ_ζ are the relaxation times for the polar and azimuthal motions. The root mean square (rms) angular dislacement for the internal motions is given by $\langle\delta\epsilon^2\rangle^{1/2}$ and $\langle\delta\zeta^2\rangle^{1/2}$. The internal motion is considered isotropic if $\langle\delta\epsilon^2\rangle = \langle\delta\zeta^2\rangle \sin^2 \epsilon_0$. Because the internal relaxation times are much faster than the rotational correlation time $\tau_\epsilon = \tau_\zeta \ll \tau_{rot}$, it is possible to set $C^i_c(t) = C^i_c(\infty)$ for all times $t \geq 500$ ps. Therefore, $C^i_c(\infty)$ also reduces to an amplitude factor in the general correlation function (eq 21). For very short DNA fragments it is reasonable to assume a rigid structure without any cooperative bending and twisting motions, and for cylindrically symmetric molecules the effective rotational correlation times can be calculated similarly to eq 12.

$$\tau_{nmr} = C^i_0(\infty)(6\Theta_\perp)^{-1} + C^i_1(\infty)(\Theta_\parallel + 5\Theta_\perp)^{-1} + C^i_2(\infty)(4\Theta_\parallel + 2\Theta_\perp)^{-1} \quad (32)$$

In contrast to the expressions from Lipari and Szabo, the reduced Wigner rotation matrix elements $[d_{m0}^{(2)}(\beta_{MD})]^2$ are included in the formulas (eq 32) for the internal correlation function $C^i_c(t)$. For a rigid rod, where $\langle\delta\epsilon^2\rangle = \langle\delta\zeta^2\rangle = 0$, the amplitude factors in eq 32 reduce to the Woessner expressions. In a study of the internal motions of longer DNA fragments (Schurr & Fujimoto, 1988) an amplitude factor $D_n(\infty)$ for the overall tumbling motion is included in the calculations. It accounts for collective bending deformations that decay much faster than the uniform tumbling mode. For the very short oligonucleotides (<12 bp long), the effect is estimated to less than 5% on the effective correlation time τ_{nmr}. For the 20-mer it might decrease the relaxation time by about 10%, but this is still within the experimental error.

In Figure 6 calculated effective correlation times (eq 32) are compared with the experimental τ_{nmr} for the various oligonucleotides. The rotational diffusion coefficients are determined by using the Tirado and Garcia de la Torre formulas

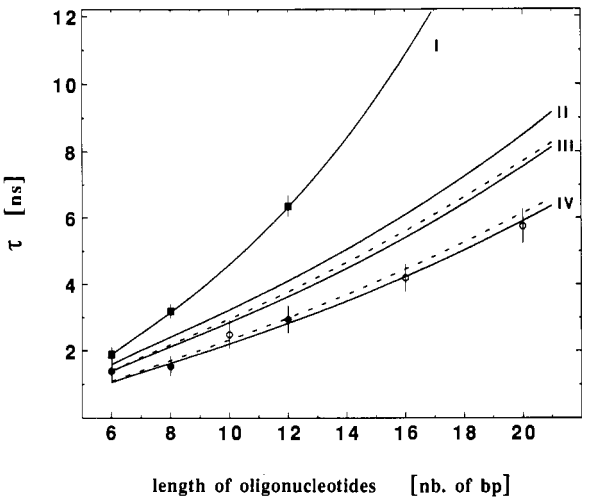

FIGURE 6: Comparison of experimental with theoretical rotational correlation times, including local internal motion of the bases. The symbols correspond to the same experimental data as in Figure 5. (I) Theoretical correlation times for the rotation of the symmetry axis ($\tau_\perp = 1/6\Theta_\perp$) from the Tirado and Garcia de la Torre formulas (eq 13). (II–IV) Corresponding values of τ_{nmr} from eq 32 including the dynamic overdamped librational motion model; the amplitude was chosen to be $\langle\delta\epsilon^2\rangle^{1/2} = 0°$ (II), 10° (III), and 18° (IV). Calculations are based on $\epsilon_0 = 90°$, a rise per base of 3.4 Å, a diameter of 20.5 Å, $T = 20$ °C, and $\eta_0 = 1.002$ cP. The broken lines above are computed with $\epsilon_0 = 70°$.

with a rise per base of 3.4 Å and a diameter of 20.5 Å. The orientation of the internuclear vector within the rod frame was varied from $\epsilon_0 = 90°$ to 70°, and the extent of librational motion was chosen as $\langle\delta\epsilon^2\rangle^{1/2} = 0°$, 10°, and 18°. Figure 6 shows that, assuming the bases are perpendicularly oriented to the helix axis, the rms amplitude of the local internal motions has to be about 18° to account for the fast correlation times measured by NMR. The effect of a base tilt with respect to the helix axis is small as long as the tilt angle does not exceed 20°. For $\epsilon_0 = 70°$ the amplitude for the librational motion would increase to about 20° to account for the fast NMR correlation times. While the effect of the local internal motion correlation function on τ_{nmr} is the dominating factor, it is obvious that to characterize the mean orientation of the bases, described by the intermolecular vector in case of the NMR experiment, a precise knowledge of the extent of internal motions of the bases is required.

The resulting angle that describes the spatial restriction of the internal motions is different for the two dynamic models applied to the experimental data, 29° in the case of the diffusion in a cone and 18° for the overdamped librations model. This is not surprising because the two models start from different premises. In the overdamped librational motion model a restoring force is assumed to restrict the internal motion, while in the cone model a diffusion coefficient characterizes the dynamics of the bases. A comparison of the two dynamic models with the same experimental data illustrates that if the model contains no sources for a restoring force as in the case of the diffusion in a cone model, a significantly larger amplitude for the librational motion of the bases is found. If one assumes that the librational motion of the bases can be described by a Gaussian distribution, the root mean square amplitude is given by $(1/2)^{1/2}\,\theta_0$ and results in $\theta_{rms} = 20.5°$. It should be emphasized that the internal motion amplitudes and relaxation rates obtained from experimental data are strongly model dependent.

Local internal motions have been extensively studied to estimate the importance of such fast conformational changes on the biological role of DNA and RNA (e.g., DNA–protein interactions). From X-ray crystallographic measurements it is evident that the coordinates of DNA show large thermal parameters (Drew et al., 1982). A "segmented rigid-body" model was used (Holbrook & Kim, 1984) to determine the internal mobility of individual subgroups from crystallographic data. It was found that the amplitude of librational motion for the bases and the ribose units amounts to ±20°. From a number of solid-state ^{2}H NMR experiments on oriented DNA fibers (DiVerdi & Opella, 1981; Shindo et al., 1987; Brandes et al., 1988a,b) and liquid crystals (Brandes & Kearns, 1988), the amplitude of the internal mobility was determined to be dependent on the degree of hydration and to increase from 4° to ≥15° with increasing water content. A recent investigation of a dodecamer (Kintanar et al., 1989) is not inconsistent with the results from higher molecular weight DNA and its sonicated fragments. The interpretation of experimental results from solution studies exhibits a larger diversity, mainly due to the appearance of overall and collective motions. The differences in the dynamic models used to interpret the data appear to be the most important reason for the differences in the conclusions drawn from the experimental results. Neglecting the influence of collective twisting and bending motions leads to a very large estimate for the amplitudes of the local librational modes of the bases. Schurr (1984) has developed a dynamic model that takes into account the collective deformation modes, and a reevaluation of experimental NMR relaxation data (Schurr & Fujimoto, 1988) results in a significantly smaller amplitude (<12°) for the local motions of the bases.

It appears to us, at least for the small DNA fragments which are almost rigid, that this latter model is not applicable. The expression for the amplitude of the uniform twisting mode $B_n(\infty)$ [see eq 25 in Schurr and Fujimoto (1988)] gives $B_0 = 0$ and leads to the conclusion that the end-over-end rotational correlation time $1/6\Theta_\perp$ does not contribute to the effective correlation time. In the case of rigid molecules with no collective twisting and bending motion present, Schurr's expression does not reduce to the Woessner formulas. Instead, it gives a significantly smaller effective relaxation time. For the small oligonucleotides studied here, calculations using Schurr's model show that the diameter has to be increased to about 26 Å to give an amplitude of ~10° for the internal motion. This would be inconsistent with the DNA fragment diameter obtained from the DDLS experiments.

Conclusion

We have combined DDLS and NMR cross-relaxation experiments to characterize the overall reorientation and internal local motion of three short oligonucleotides with different structure. DDLS gives correlation times for the end-over-end rotation that are in very good agreement with theoretical values from the Tirado and Garcia de la Torre theory for cylindrically symmetric molecules. This theory uses hydrodynamic stick boundary conditions. It is the only theory that predicts the transport coefficients for cylindrical molecules with very small axial ratios and is in many cases preferable to the Perrin equations because the shapes of some small biomolecules, especially short oligonucleotides, resemble a cylinder more closely than an ellipsoid.

The rotational correlation times provided by DDLS for oligonucleotides of different conformation but almost the same number of base pairs are significantly different. The method is sensitive enough to allow one to very easily distinguish between the standard double-helical and hairpin structures. For the same double-helical conformation the rotational correlation times are a very sensitive measure of the molecular

length, and the Tirado and Garcia de la Torre hydrodynamic theory provides a powerful method for calculating the corresponding dimensions. In comparison to other experimental methods, DDLS has the advantage that it introduces no significant disturbances to the sample, requires only that the molecules exhibit an optical anisotropy, and can be generally performed at lower concentrations than NMR measurements.

The light scattering data provide a solid basis for interpreting the NMR results with respect to local internal motions of the bases. The correlation times from the cross-relaxation measurements are significantly smaller than those from the predictions of the Tirado and Garcia de la Torre theory for rigid rodlike molecules. Within the experimental error the extent of local internal motion is independent of the length and base sequence of the studied oligonucleotides. The dynamic models used to characterize the internal wobbling of the bases give amplitudes of the librational motion between 18° (overdamped librational motion) and 29° (diffusion in a cone), which gives $\theta_{rms} = 20.5°$. It is assumed that the tilt angle lies between 0° and 20°. Unfortunately, both parameters, the orientation of the bases (or more precisely of the internuclear vector in NMR) and the amplitude of the internal motion, are interconnected, and in solution could not be observed separately by any of the methods used so far. A comparison with calculations from crystallographic data and results from solid-state experiments indicate that the amplitude of the librational motion of the bases does not change drastically in solution (assuming that the motion is adequately described by the dynamic models that were applied to the experimental data).

We have shown that DDLS and NMR relaxation measurements are valuable complements to each other in characterizing the structure and dynamics of short DNA fragments. While the light scattering experiment is a sensitive probe of conformational changes that result in a change of the overall size and shape of the molecule, the NMR experiment gives valuable additional information about local dynamics. Due to the complex origin of the NMR signal, knowledge of the overall reorientation relaxation time provided by DDLS makes the interpretation of the NMR results more definite. When used together, the methods provide a powerful tool for detecting and understanding the conformational and dynamic characteristics of short DNA fragments.

Acknowledgments

W.E. thanks the Alexander von Humboldt foundation for award of a Feodor-Lynen fellowship. The 500-MHz NMR spectrometer was funded by grants from the National Science Foundation (DMB-8515942) and the National Institutes of Health (1-51-RR2733-01).

Registry No. $d(CG)_4$, 89991-79-7; $d(CG)_6$, 92950-48-6; d-(CGCGTTGTTCGCG), 115427-43-5.

References

Abragam, A. (1978) *The Principles of Nuclear Magnetism*, Chapter VIII, Clarendon Press, Oxford, U.K.

Assa-Munt, N., Granot, J., Behling, R. W., & Kearns, D. R. (1983) *Biochemistry 23*, 944–955.

Barkley, M. D., & Zimm, B. H. (1979) *J. Chem. Phys. 70*, 2991–3007.

Berne, B. J., & Pecora, R. (1976) *Dynamic Light Scattering*, Wiley, New York.

Bobst, A. M., Kao, S.-C., Toppin, R. C., Ireland, T. C., & Thomas, I. E. (1984) *J. Mol. Biol. 173*, 63–74.

Bolton, P. H., & James, T. L. (1980a) *J. Phys. Chem. 83*, 3359–3366.

Bolton, P. H., & James, T. L. (1980b) *Biochemistry 19*, 1388–1392.

Borgias, B. A., & James, T. L. (1988) *J. Magn. Reson. 79*, 493–512.

Brandes, R., & Kearns, D. R. (1988) *J. Phys. Chem. 92*, 6836–6841.

Brandes, R., Vold, R. R., Vold, R. L., & Kearns, D. R. (1986) *Biochemistry 25*, 7744–7751.

Brandes, R., Vold, R. R., & Kearns, D. R. (1988) *J. Mol. Biol. 202*, 321–332.

Brink, D. M., & Satchler, G. R. (1968) *Angular Momentum*, Clarendon Press, Oxford, U.K.

Broersma, S. (1960a) *J. Chem. Phys. 32*, 1626–1631.

Broersma, S. (1960b) *J. Chem. Phys. 32*, 1632–1635.

Broersma, S. (1980) *J. Chem. Phys. 74*, 6889–6890.

Charney, E., Chen, H. H., Henry, E. R., & Rau, D. C. (1986) *Biopolymers 25*, 885–904.

CRC Handbook of Chemistry and Physics (1980) 60th ed., CRC Press, Boca Raton, FL.

DiVerdi, J. A., & Opella, S. J. (1981) *J. Mol. Biol. 149*, 307–311.

Dote, J. L., & Kivelson, D. (1983) *J. Phys. Chem. 87*, 3889–3993.

Drew, H. R., Samson, S., & Dickerson, R. E. (1982) *Proc. Natl. Acad. Sci. U.S.A. 79*, 4040–4044.

Early, T. A., & Kearns, D. R. (1979) *Proc. Natl. Acad. Sci. U.S.A. 76*, 4165–4169.

Edmondson, S. P., & Johnson, W. C., Jr. (1985) *Biopolymers 24*, 825–841.

Edmondson, S. P., & Johnson, W. C., Jr. (1986) *Biopolymers 25*, 2335–2348.

Edmondson, S. P., & Johnson, W. C., Jr. (1987) *Biopolymers 26*, 1941–1956.

Eimer, W. (1987) Ph.D. Thesis, University of Bielefeld.

Elias, J. G., & Eden, D. (1981) *Biopolymers 20*, 2368–2380.

Genest, D., & Wahl, Ph. (1978) *Biochim. Biophys. Acta 521*, 502–509.

Hård, T. (1987) *Biopolymers 26*, 613–618.

Hård, T., & Kearns, D. R. (1986) *Biopolymers 25*, 1519–1529.

Hogan, M. E., & Jardetzky, O. (1980) *Biochemistry 19*, 3460–3468.

Hogan, M., Dattagupta, N., & Crothers, D. M. (1979) *Proc. Natl. Acad. Sci. U.S.A. 75*, 195–199.

Holbrook, S. R., & Kim, S.-H. (1984) *J. Mol. Biol. 173*, 361–388.

Hu, C. M., & Zwanzig, R. (1974) *J. Chem. Phys. 60*, 4354–4357.

Huntress, W. T., Jr. (1968) *J. Chem. Phys. 48*, 3524–3533.

Ikuta, S., Chattopadhyaya, R., Ito, H., Dickerson, R. E., & Kearns, D. R. (1986) *Biochemistry 25*, 4840–4849.

Kao, S.-C., & Bobst, A. M. (1985) *Biochemistry 24*, 5465–5469.

Kintanar, A., Huang, W.-C., Schindele, D. C., Wemmer, D. E., & Drobny, G. (1989) *Biochemistry 28*, 282–293.

Kivelson, D. (1987) in *Rotational Dynamics of Small and Macromolecules* (Dorfmüller, T., & Pecora, R., Eds.) Springer-Verlag, Heidelberg.

Koenig, S. H. (1975) *Biopolymers 14*, 2421–2423.

Lane, A. N., Lefevre, J.-F., & Jardetzky, O. (1986) *J. Magn. Reson. 66*, 201–218.

Lee, C.-H., & Charney, E. (1982) *J. Mol. Biol. 161*, 289–303.

Lipari, G., & Szabo, A. (1981) *J. Chem. Phys. 75*, 2971–2976.

Lipari, G., & Szabo, A. (1982a) *J. Am. Chem. Soc. 104*, 4546–4559.

Lipari, G., & Szabo, A. (1982b) *J. Am. Chem. Soc. 104*, 4559-4570.
Magde, D., Zappala, M., Knox, W. H., & Nordlund, T. H. (1983) *J. Chem. Phys. 87*, 3286-3288.
Millar, D. P., Robbins, R. J., & Zewail, A. H. (1981) *J. Chem. Phys. 76*, 2080-2094.
Millero, F. J., Dexter, R., & Hoff, E. (1971) *J. Chem. Eng. Data 16*, 85-87.
Mirau, P. A., & Kearns, D. R. (1983) *Biochemistry 23*, 5439-5446.
Mirau, P. A., Behling, R. W., & Kearns, D. R. (1985) *Biochemistry 24*, 6200-6211.
Perrin, F. (1934) *J. Phys. Radium 5*, 497-510.
Perrin, F. (1936) *J. Phys. Radium 7*, 1-11.
Saenger, W. (1984) *Principles of Nucleic Acid Structure*, Springer-Verlag, New York.
Schurr, J. M. (1984) *Chem. Phys. 84*, 71-96.
Schurr, J. M., & Fujimoto, B. S. (1988) *Biopolymers 27*, 1543-1569.
Shindo, H., Hiyama, Y., Siddhartha, R., Cohen, J. S., & Torchia, D. A. (1987) *Bull. Chem. Soc. Jpn. 60*, 1631-1640.
Spiess, H. W. (1978) Dynamic NMR Spectroscopy, *Basic Princ. Prog. NMR 15*, 54-214.
Tirado, M. M., & Garcia de la Torre, J. (1979) *J. Chem. Phys. 71*, 2581-2587.
Tirado, M. M., & Garcia de la Torre, J. (1980) *J. Chem. Phys. 73*, 1986-1993.
Tirado, M. M., Lopez Martinez, M. C., & Garcia de la Torre, J. (1984a) *J. Chem. Phys. 81*, 2047-2052.
Tirado, M. M., Lopez Martinez, M. C., & Garcia de la Torre, J. (1984b) *Biopolymers 23*, 611-615.
van Cittert, P. H. (1931) *Z. Phys. 69*, 298.
Wang, C. C., & Pecora, R. (1980) *J. Chem. Phys. 72*, 5333-5340.
Williamson, J. R. (1988) Ph.D. Thesis, Stanford University.
Williamson, J. R., & Boxer, S. G. (1989) *Biochemistry 28*, 2819-2831.
Woessner, D. E. (1962) *J. Chem. Phys. 37*, 647-654.
Wu, P., Fujimoto, B. S., & Schurr, J. M. (1987) *Biopolymers 26*, 1463-1488.
Wüthrich, K. (1986) *NMR of Proteins and Nucleic Acids*, Wiley, New York.
Yoshizaki, T., & Yamakawa, H. (1980) *J. Chem. Phys. 72*, 57-69.
Youngren, G. K., & Acrivos, A. (1976) *J. Chem. Phys. 63*, 3846-3848.

Synthesis and Characterization of *trans*-[$Pt(NH_3)_2Cl_2$] Adducts of d(CCTCGAGTCTCC)·d(GGAGACTCGAGG)†

Christopher A. Lepre, Laurent Chassot, Catherine E. Costello, and Stephen J. Lippard*
Department of Chemistry, Massachusetts Institute of Technology, Cambridge, Massachusetts 02139
Received May 24, 1989; Revised Manuscript Received August 29, 1989

ABSTRACT: The reaction of *trans*-diamminedichloroplatinum(II) (*trans*-DDP), the inactive isomer of the anticancer drug cisplatin, with the single-stranded deoxydodecanucleotide d(CCTCGAGTCTCC) in aqueous solution at 37 °C was monitored by reversed-phase HPLC. Consumption of the dodecamer follows pseudo-first-order reaction kinetics with a rate constant of 1.25 (4) × 10^{-4} s^{-1}. Two intermediates, shown to be monofunctional adducts in which Pt is coordinated to the guanine N7 positions, were trapped with $NH_4(HCO_3)$ and identified by enzymatic degradation analysis. These monofunctional adducts and a third, less abundant, one are rapidly removed from the DNA by thiourea under mild conditions. When allowed to react further, the monofunctional intermediates formed a single main product that was characterized by ^1H NMR spectroscopy and enzymatic digestion as the bifunctional 1,3-intrastrand cross-link *trans*-[$Pt(NH_3)_2${d(CCTCGAGTCTCC)-*N7-G(5)*,*N7-G(7)*}]. Binding of the *trans*-$\{Pt(NH_3)_2\}^{2+}$ moiety to the guanosine N7 positions decreases the pK_a at N1 and leads to destacking of the intervening A(6) base. The double-stranded *trans*-DDP-modified and unmodified DNAs were obtained by annealing the complementary strand to the corresponding single strands and then studied by ^{31}P and ^1H NMR and UV spectroscopy. *trans*-DDP binding does not induce large changes in the O–P–O bond or torsional angles of the phosphodiester linkages in the duplex, nor does it significantly alter the UV melting temperature. *trans*-DDP binding does, however, cause the imino protons of the platinated duplex to exchange rapidly with solvent by 50 °C, a phenomenon that occurs at 65 °C for the unmodified duplex. A structural model for the platinated double-stranded oligonucleotide was generated through molecular dynamics calculations. This model reveals that the *trans*-DDP bifunctional adduct can be accommodated within the double helix with minimal distortion of the O–P–O angles and only local disruption of base pairing and destacking of the platinated bases. The model also predicts hydrogen bond formation involving coordinated ammine ligands that bridge the two strands.

The anticancer drug *cis*-diamminedichloroplatinum(II) (cisplatin, or *cis*-DDP) binds to DNA, inactivating it as a template for replication and transcription [for reviews see Pinto and Lippard (1985a), Lippard (1987), Reedijk (1987), Eastman (1987), Sherman and Lippard (1987) and Roberts (1988)]. The clinically ineffective trans isomer also binds DNA, forming adducts that terminate replication both in vivo

† We thank the Swiss National Science Foundation for a Postdoctoral Fellowship (to L.C.).

0006-2960/90/0429-811$02.50/0